Author(s): Konu, Jari; Tuononen, Heikki; Chivers, Tristram; Corrente, Andrea; Boeré, René; Roemmele, Tracey

Title: In Search of the [PhB(μ-NtBu)2]2As• Radical: Experimental and Computational Investigations of the Redox Chemistry of Group 15 Bis-boraamidinates

Year: 2008

Version:

Please cite the original version:

Konu, J., Tuononen, H., Chivers, T., Corrente, A., Boeré, R., & Roemmele, T. (2008). In Search of the [PhB(μ-NtBu)2]2As• Radical: Experimental and Computational Investigations of the Redox Chemistry of Group 15 Bis-boraamidinates. Inorganic Chemistry, 47(9), 3823-3831. https://doi.org/10.1021/ic702435e

In Search of the $[PhB(\mu\text{-}N^tBu)_2]_2As^{\bullet}$ Radical: Experimental and Computational Investigations of the Redox Chemistry of Group 15 Bis-boraamidinates

Jari Konu,[†] Heikki M. Tuononen,[‡] Tristram Chivers,[†]* Andrea M. Corrente,[†] René T. Boeré[§] and Tracey L. Roemmele[§]

[†] *Department of Chemistry, University of Calgary, Calgary, Alberta T2N 1N4, Canada*

[‡] *Department of Chemistry, University of Jyväskylä, P.O. Box 35, Jyväskylä, FI-40014, Finland*

[§] *Department of Chemistry and Biochemistry, University of Lethbridge, Lethbridge, Alberta T1K 3M4, Canada*

[*] To whom correspondence should be addressed.
Telephone: (403) 220-5741
Fax: (403) 289-9488
E-mail: chivers@ucalgary.ca

Abstract

DFT calculations for the group 15 radicals $[PhB(\mu\text{-}N^tBu)_2]_2M^\bullet$ (M = P, As, Sb, Bi) predict a pnictogen-centered SOMO with smaller contributions to the unpaired spin density arising from the nitrogen and boron atoms. The reactions of $Li_2[PhB(\mu\text{-}NR)_2]$ (R = ^{t}Bu, Dipp) with PCl_3 afforded the unsolvated complex $LiP[PhB(\mu\text{-}N^tBu)_2]_2$ (**1a**) in low yield and $ClP[PhB(\mu\text{-}NDipp)_2]$ (**2**) both of which were structurally characterized. Efforts to produce the arsenic-centered neutral radical, $[PhB(\mu\text{-}N^tBu)_2]_2As^\bullet$, via oxidation of $LiAs[PhB(\mu\text{-}N^tBu)_2]_2$ with one-half equivalent of SO_2Cl_2 yielded the Zwitterionic compound, $[PhB(\mu\text{-}N^tBu)_2As(\mu\text{-}N^tBu)_2B(Cl)Ph]$ (**3**), containing one four-coordinate boron center with a B-Cl bond. The reaction of **3** with $GaCl_3$ produced the ion-separated salt, $[PhB(\mu\text{-}N^tBu)_2]_2As^+GaCl_4^-$ (**4**), which was characterized by X-ray crystallography. The reduction of **3** with sodium naphthalenide occurred by a two-electron process to give the corresponding anion $[\{PhB(\mu\text{-}N^tBu)_2\}_2As]^-$ as the sodium salt. Voltammetric investigations of **4** and $LiAs[PhB(\mu\text{-}N^tBu)_2]_2$ (**1b**) revealed irreversible processes. Attempts to generate the neutral radical $[PhB(\mu\text{-}N^tBu)_2]_2As^\bullet$ from these ionic complexes via in situ electrolysis did not produce an EPR-active species.

Introduction

The dianionic boraamidinate (*bam*) ligand, $[RB(NR')_2]^{2-}$, is formally isoelectronic with the extensively studied monoanionic amidinate (*am*) ligand $[RC(NR')_2]^-$. Recent work on early main group and transition-metal complexes has established that the 2- charge on the *bam* ligand results in some interesting fundamental differences compared to the behavior of the monoanionic *am* ligand. The 2- charge lowers the requirement for ancillary ligands around high oxidation-state metal centers. Consequently, homoleptic species of the type $[ML_2]^{x-}$ (x = 0,1,2) and $[ML_3]^{2-}$ (L = *bam*) are common features of main group and transition-metal complexes.[1-3] Perhaps the most intriguing consequence of the 2- charge is the facile tendency for redox transformations to occur in which the the $[bam]^{2-}$ dianion is oxidized to the corresponding monoanion radical $[bam]^{-\bullet}$. This paramagnetic ligand can be stabilized through chelation, *e.g.* to early main-group metals.[3-5] In the case of certain Group 13 metals it has been possible to isolate, *stable* neutral radicals, for example the highly colored spirocyclic systems $\{M[PhB(\mu\text{-}N^tBu)_2]_2\}^\bullet$ (M = Al, Ga) and determine their X-ray structures.[4] The SOMO in these radicals is located primarily and equally in p-orbitals on the four nitrogen atoms of the two *bam* ligands; there is very little unpaired electron density on the Group 13 centers. The corresponding boron and indium-containing radicals $\{M[PhB(\mu\text{-}N^tBu)_2]_2\}^\bullet$ (M = B, In) were characterized in solution by EPR spectroscopy.[5] However, the indium radical is not sufficiently stable to be isolated in the solid state, while the boron analogue, although it is thermally very stable, could not be obtained in a pure form.

In a recent investigation we reported the first examples of heavy Group 15 boraamidinates in which the versatile coordinating ability of the *bam* ligand was highlighted.[6] In addition to the mono-*bam*s $ClM[PhB(\mu\text{-}N^tBu)_2]$ (**A**; M = As, Sb, Bi) with a potentially useful M-Cl reactive site, the unusual 2:3 *bam* complexes, $M_2[PhB(\mu\text{-}N^tBu)_2]_3$ (**B**; M = Sb, Bi), displayed a unique bonding arrangement in which two metal centers are each *N*,*N*′-chelated by one *bam* ligand and the two

[M(*bam*)]$^{+}$ units are bridged by the third [*bam*]$^{2-}$ ligand. For the 1:2 Group 15 *bam* systems, both solvated complexes (Et_2O)LiM[PhB(μ-N^{t}Bu)$_2$]$_2$ (**C;** M = As, Bi) and unsolvated ladder structures LiM[PhB(μ-N^{t}Bu)$_2$]$_2$ (**D**; M = As, Sb) were observed; these complexes showed interesting fluxional behavior in solution (Berry pseudorotation) in the case of M = Sb, Bi.[6] Although monofunctional phosphorus-containing *bam* complexes of the type XP[PhB(μ-N^{t}Bu)$_2$] (X = Cl, Br; type **A**) are known,[7] a bis-*bam* complex LiP[PhB(μ-N^{t}Bu)$_2$]$_2$ (type **C** or **D**) has not been reported.

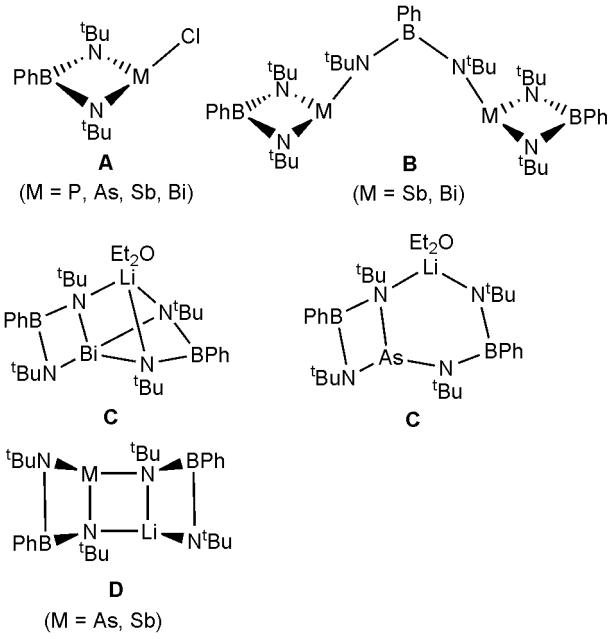

In the current study we were primarily interested in radicals of the type {M[PhB(μ-N^{t}Bu)$_2$]$_2$}$^{\bullet}$ (M = Group 15 element) in order to determine the effect of the additional pair of electrons on the molecular and electronic structures of the Group 15 systems in comparison with those of the well-characterized Group 13 analogs (M = Al, Ga).[4,5] In this context we report (a) the results of DFT calculations of the molecular structures and EPR parameters of the pnictogen-centred radicals[7] [PhB(μ-NR)$_2$]$_2$M$^{\bullet}$ (M = P, As, Sb, Bi; R = Me, ^{t}Bu) (b) the synthesis and X-ray structures of LiP[PhB(μ-N^{t}Bu)$_2$]$_2$ (**1a**) and ClP[PhB(μ-NDipp)$_2$]$_2$ (**2**) (c) the synthesis and X-ray structures of the Zwitterionic complex [PhB(μ-N^{t}Bu)$_2$As(μ-N^{t}Bu)$_2$B(Cl)Ph] (**3**) and the ion-separated salt [PhB(μ-

$N^tBu)_2]_2As^+GaCl_4^-$ (**4**) (d) the chemical reduction of **3** and the cation $[PhB(\mu\text{-}N^tBu)_2]_2As^+$, and (e) voltammetric studies of the bis(boraamidinate)arsenic system.

Experimental Section

General Procedures. All reactions and the manipulations of products were performed under an argon atmosphere by using standard Schlenk techniques or an inert atmosphere glove box. The compounds $PhBCl_2$ (Aldrich, 97%), $GaCl_3$ (Aldrich, 99.99%), $AsCl_3$ (Alfa, 99%), $[^nBu_4N]Br_3$ (Aldrich, 98%) and $NO[SbF_6]$ (Aldrich, 99.9%) were used as received. PCl_3 (Aldrich, 99%) was distilled prior to use. $LiN(H)^tBu$ was prepared by the addition of ^{n}BuLi to a solution of anhydrous $^t BuNH_2$ in *n*-hexane at -10 ^{o}C and its purity was checked by ^{1}H NMR spectroscopy. The compounds $PhB[N(H)^tBu]_2$,[8a] $Li_2[PhB(\mu\text{-}N^tBu)_2]$,[8a] $Li_2[PhB(\mu\text{-}NDipp)_2]$[8b] and $LiAs[PhB(\mu\text{-}N^tBu)_2]_2$[6] (**1b**) were prepared as described earlier. The solvents *n*-hexane, toluene, Et_2O and THF were dried by distillation over Na/benzophenone, and the solvents dichloromethane and acetonitrile were distilled from CaH_2 under an argon atmosphere prior to use. Electrochemical grade tetrabutylammonium hexafluorophosphate $[^nBu_4N][PF_6]$ (Fluka) was used as the supporting electrolyte and was kept in a dessicator prior to use. Ferrocene, prepared following the procedure described by Jolly,[9] was sublimed prior to use. Elemental analyses were performed by Analytical Services, Department of Chemistry, University of Calgary and Canadian Microanalytical Service Ltd., Vancouver, British Columbia.

Spectroscopic Methods. The ^{1}H, ^{7}Li, ^{11}B, ^{13}C, ^{31}P and ^{71}Ga NMR spectra were obtained in CD_2Cl_2, d_8-THF or d_8-toluene at 23 ^{o}C on a Bruker DRX 400 spectrometer operating at 399.59, 155.30, 128.20, 100.49, 161.77 and 121.87 MHz, respectively. ^{1}H and ^{13}C spectra are referenced to the solvent signal and the chemical shifts are reported relative to $(CH_3)_4Si$. ^{7}Li and ^{11}B NMR spectra are referenced externally and the chemical shifts are reported relative to a 1.0 M solution of LiCl in

D_2O and to a solution of $BF_3{\cdot}Et_2O$ in C_6D_6, respectively. Similarly, ^{31}P and ^{71}Ga NMR spectra are referenced externally and the chemical shifts are reported relative to an 85% solution of H_3PO_4 and to a solution of $Ga(NO_3)_3$ in D_2O, respectively.

Electrochemical Methods and Procedures. Cyclic voltammograms (CVs) were obtained at temperatures of 21 ± 2°C in acetonitrile, dichloromethane and tetrahydrofuran solutions containing 0.1 M, 0.4 M, and 0.4 M $[^nBu_4N][PF_6]$ respectively, as the supporting electrolyte. CVs were executed by using a PARSTAT 2273 computer-controlled potentiostat with PowerSuite (v.2.58) software. The cell design consisted of a conventional three electrode set-up with a 3.0 mm diameter glassy-carbon (GC), a 1.6 mm diameter platinum (Pt), or a 1.6 mm diameter gold (Au) working electrode, a Pt wire auxiliary and a silver wire quasi-reference electrode. The reference electrode was separated from the bulk solution by a fine-porosity frit. CVs were obtained over scan rates of 0.1 – 20 V s^{-1}. All potentials are reported vs. the operative formal potential, $E^{0/}_{Fc^{+/0}}$, for the Fc^+/Fc redox couple (Fc = ferrocene), which was used as an internal standard. The electrodes were polished with 0.05 micron alumina on a clean polishing cloth (Buehler, USA), rinsed with distilled water, and dried with tissue paper prior to use. The solution was purged with dry nitrogen for 10 min directly before use, and a blanket of nitrogen gas covered the solution during all experiments. The cell design for all Simultaneous Electrochemical Electron Paramagnetic Resonance (SEEPR) experiments has been described previously.[10] This cell was placed inside a Bruker EMX 113 spectrometer operating at X-band frequencies (9.8 GHz) at 18 ± 2 °C.

X-ray Crystallography. Crystals of $LiP[PhB(\mu\text{-}N^tBu)_2]_2$ (**1a**), $ClP[PhB(\mu\text{-}NDipp)_2]$ (**2**), $[PhB(\mu\text{-}N^tBu)_2As(\mu\text{-}N^tBu)_2B(Cl)Ph]$ (**3**) and $[PhB(\mu\text{-}N^tBu)_2]_2As(GaCl_4)$ (**4**) were coated with Paratone 8277 oil and mounted on a glass fiber. Diffraction data were collected on a Nonius KappaCCD diffractometer using monochromated MoK_α radiation (λ = 0.71073 Å) at -100 °C. The data sets were corrected for Lorentz and polarization effects, and empirical absorption correction

was applied to the net intensities. The structures were solved by direct methods using SHELXS-97 [11] and refined using SHELXL-97.[12] After the full-matrix least-squares refinement of the non-hydrogen atoms with anisotropic thermal parameters, the hydrogen atoms were placed in calculated positions [C-H = 0.98 Å for $C(CH_3)_3$ and 0.95 Å for phenyl hydrogens]. The isotropic thermal parameters of the hydrogen atoms were fixed at 1.2 times to that of the corresponding carbon for phenyl hydrogens, and 1.5 times for $C(CH_3)_3$. In the final refinement the hydrogen atoms were riding on their respective carbon atoms.

Similarly to the structures of $LiM[PhB(\mu\text{-}N^tBu)_2]_2$ (M = As, Sb),[6] the lithium and phosphorus atom positions in the structure of **1a** were disordered with the atoms distributed over the two atomic sites. The two atoms were not constrained to locate in the same position, but the anisotropic thermal parameters were restricted to be equal. The site occupation factors were fixed to be 50% for these atoms. The crystal structure of **4** exhibits two discrete ion pairs in which the second $GaCl_4^-$ anion shows disorder in the chlorine atom positions. In the final refinement, the site occupation factors for these atoms were approximately 80/20 %. The scattering factors for the neutral atoms were those incorporated with the programs. Crystallographic data are summarized in Table 1.

Computational Details. The geometries of all studied compounds were optimized by using DFT. The calculations utilized both the hybrid PBE0 exchange-correlation functional for Me substituted systems as well as its non-hybrid GGA variant PBEPBE for ^{t}Bu substituted systems.[13] Ahlrichs' triple-zeta valence basis sets augmented by one set of polarization functions (TZVP) were employed in all calculations.[14] For heavy atoms antimony and bismuth, the corresponding ECP basis sets were used.[14, 15] Appropriate molecular point groups and the resolution-of-the-identity approximation were used to improve the efficiency of the calculations. Geometry optimizations were done with Turbomole 5.9.1[16] (R = ^{t}Bu) and Gaussian 03[17] (R = Me) program packages.

Hyperfine coupling constants were calculated for all paramagnetic systems in their geometry-optimized structures by using both a non-relativistic and a scalar relativistic (ZORA) approach[18] within the unrestricted Kohn-Sham formalism. The non-relativistic calculations utilized the same basis sets as the geometry optimizations, but only the hybrid version of the PBEPBE functional was employed. However, for the heavier nuclei antimony and bismuth, the use of ECP basis sets prevents the direct determination of hyperfine couplings using the same method. In addition, relativistic calculations are essential in order to obtain more than a qualitative accuracy for systems containing heavy nuclei. Thus, relativistic calculations for systems with Sb and Bi atoms were carried out. The calculations utilized the PBEPBE GGA functional[13] together with the large TZ2P STO-type basis sets.[19] The hyperfine coupling constant calculations were done with the Gaussian 03[17] (non-relativistic) and ADF 2007.01[20] program packages (relativistic). The values reported in Table 2 are non-relativistic for the lighter nuclei and scalar-relativistic for the heavier atoms antimony and bismuth.

Synthesis of LiP[PhB(μ-N^{t}Bu)$_2$]$_2$ (1a). A solution of Li_2[PhB(μ-N^{t}Bu)$_2$] (0.244 g, 1.00 mmol) in 15 mL of Et_2O was added to a solution of PCl_3 (0.069 g, 0.50 mmol) in 15 ml of Et_2O at -80 ^{o}C. The reaction mixture was stirred for ½ h at -80 ^{o}C and 16 h at 23 ^{o}C. LiCl was removed by filtration and the solvent was concentrated to *ca.* 2 ml. Crystallization from diethyl ether afforded **1a** after 5 days at 5 ^{o}C (0.062 g, 25%). ^{1}H NMR (toluene-d$_8$, 23 ^{o}C): δ 6.16-7.70 [m, 10H, C$_6$*H*$_5$], 1.46 [d, $^4J(^1H,^{31}P)$ = 2.4 Hz, 9H, C(C*H*$_3$)$_3$], 1.34 [s, 18H, C(C*H*$_3$)$_3$], 1.16 [s, 9H, C(C*H*$_3$)$_3$]. ^{11}B NMR: δ 34.9. ^{7}Li NMR: δ 0.94. ^{31}P{^{1}H} NMR: δ 87.1.[21]

Synthesis of ClP[PhB(μ-NDipp)$_2$]$_2$ (2). A solution of Li_2[PhB(μ-NDipp)$_2$] (0.726 g, 1.60 mmol) in Et_2O (30 mL) was added to a solution of PCl_3 (0.14 mL, 1.60 mmol) in Et_2O (10 mL) at -80°C. The reaction mixture was stirred for ½ h at -80 ^{o}C and 18 h at 23 ^{o}C. The volatiles were removed *in vacuo* and the product was then extracted with *n*-hexane. The precipitate of LiCl was

removed by filtration and the solvent was evaporated under vacuum yielding an oily product that solidified to give a pale yellow powder of **2** after 24 h at 23 °C (0.648 g, 1.30 mmol, 80%). Anal. Calcd. for $C_{30}H_{39}BN_2PCl$: C, 71.37; H, 7.78; N, 5.55. Found: C, 71.35; H, 8.24; N, 5.45. ^{1}H NMR (toluene-d_8, 23°C): δ 7.26-6.37 [m, 11H, aromatic], 4.18 [sept., 2H, -C*H*$(CH_3)_2$ of Dipp groups, $^3J(^1H,^1H)$ = 6.8 Hz], 3.64 [2H, -C*H*$(CH_3)_2$ of Dipp groups, $^3J(^1H,^1H)$ = 6.8 Hz], 1.37 [d, 6H, -CH(C*H*$_3)_2$ of Dipp groups, $^3J(^1H,^1H)$ = 6.8 Hz], 1.27 [d, 6H, -CH(C*H*$_3)_2$ of Dipp groups, $^3J(^1H,^1H)$ = 6.8 Hz], 1.16 [d, 6H, -CH(C*H*$_3)_2$ of Dipp groups, $^3J(^1H,^1H)$ = 6.8 Hz], 1.06 [d, 6H, -CH(C*H*$_3)_2$ of Dipp groups, $^3J(^1H,^1H)$ = 6.8 Hz]. $^{13}C\{^1H\}$ NMR: δ 147.9 [d, $^2J(^{13}C,^{31}P)$ = 7.6 Hz], 145.8 [d, $^2J(^{13}C,^{31}P)$ = 6.0 Hz], 134.7, 134.5 [d, $^3J(^{13}C,^{31}P)$ = 14.8 Hz], 132.2, 128, 127.7, 124.4, 29.72 [d, $^4J(^{13}C,^{31}P)$ = 26.4 Hz], 28.76, 25.32 [d, $^4J(^{13}C,^{31}P)$ = 16.8 Hz], 24.78, 24.5, 23.98. ^{11}B NMR: δ 32.8. $^{31}P\{^1H\}$ NMR: δ 189.8. Colorless crystals of **2** were grown from *n*-hexane after 5 d at 5 °C.

Synthesis of [PhB(*μ*-N^{t}Bu)$_2$As(*μ*-N^{t}Bu)$_2$B(Cl)Ph] (3). A solution of **1b** (0.271 g, 0.50 mmol) in diethyl ether (25 mL) was cooled to -80 °C and a solution of SO_2Cl_2 (0.040 mL, 0.067 g, 0.50 mmol) in diethyl ether (1.0 mL) was added via syringe. The reaction mixture was stirred for ½ h at -80 °C and *ca.* 4 h at room temperature. LiCl was removed by filtration and the solvent was evaporated under vacuum to give **3** as a white solid (0.243 g, 85%). ^{1}H NMR (toluene-d_8, 23 °C): δ 6.98-8.24 [m, 10H, C_6H_5], 1.43 [s, 18H, C(C*H*$_3)_3$], 1.33 [s, 9H, C(C*H*$_3)_3$], 1.25 [s, 9H, C(C*H*$_3)_3$]. $^{13}C\{^1H\}$ NMR: δ 126.7-131.1 [C_6H_5], 55.6 [s, *C*$(CH_3)_3$], 55.0 [s, *C*$(CH_3)_3$], 54.3 [s, *C*$(CH_3)_3$], 32.7 [s, C(*C*$H_3)_3$], 32.6 [s, C(*C*$H_3)_3$], 32.5 [s, C(*C*$H_3)_3$]. ^{11}B NMR: δ 37.3, 7.6 ppm. Colorless crystals of **3** were obtained from Et_2O after 8 d at 5 °C.[21]

Synthesis of [PhB(*μ*-N^{t}Bu)$_2$]$_2$As$^+$GaCl$_4^-$ (4). A solution of **3** (0.285 g, 0.50 mmol) in diethyl ether (20 mL) was cooled to -80 °C and a solution of $GaCl_3$ (0.088 g, 0.50 mmol) in diethyl ether (10 mL) was added via cannula. The reaction mixture was stirred for ½ h at -80 °C and *ca.* 2 h at room temperature. The precipitate was allowed to settle and the solvent was decanted via cannula.

The product was then washed with Et_2O (2 x 20 mL) and dried under vacuum giving **4** as a white, spectroscopically pure powder (0.306 g, 82%). ^{1}H NMR (CD_2Cl_2, 23 ^{o}C): δ 7.51-7.56 [m, 10H, C_6H_5], 1.44 [s, 36H, $C(CH_3)_3$]. $^{13}C\{^1H\}$ NMR: δ 129.0-131.0 [C_6H_5], 57.7 [$C(CH_3)_3$], 32.3 [$C(CH_3)_3$]. ^{11}B NMR: δ 37.8. ^{71}Ga NMR: δ 249.6. Colorless crystals of **4** were obtained from *n*-hexane layered on top of the THF solution after 24 h at 5 ^{o}C.[21]

Results and Discussion

DFT Calculations of the Neutral Radicals [PhB(*μ*-NR)$_2$]$_2$M$^\bullet$ (M = P, As, Sb, Bi; R = Me, ^{t}Bu). Our earlier DFT calculations on the model Group 13 radicals [PhB(*μ*-NMe)$_2$]$_2$M$^\bullet$ (M = B, Al, Ga, In) revealed spirocyclic structures with spin density equally distributed over the two *bam* ligands and the SOMO distributed equally over p-orbitals on each of the four nitrogen atoms.[4, 5] By contrast, DFT calculations for the corresponding Group 15 systems [PhB(*μ*-NMe)$_2$]$_2$M$^\bullet$ predict two different types of electronic structures. For the lighter Group 15 bis-*bam*s (M = P, As, Sb) the calculations reveal a distorted C_2 symmetric trigonal bipyramidal geometry with the SOMO located primarily on the Group 15 center (Figure 1a). For the bismuth-containing bis-*bam* radical, the calculations predict a highly distorted C_1 symmetric structure with one long (2.51 Å) and one short (2.16 Å) Bi-N bond as well as a SOMO which is mainly located on the nitrogen atoms of one of the two chelating *bam*-ligands (Figure 1b). As a consequence, large (several hundred Gauss) hyperfine coupling constants for the Group 15 center are expected in the EPR spectra of the pnictogen-centered radicals [PhB(*μ*-NMe)$_2$]$_2$M$^\bullet$ (M = P, As and Sb).[7] In contrast, the EPR spectra of the analogous bismuth species should display at least ten orders of magnitude smaller Bi coupling.

Interestingly, calculations done for the more realistic N^{t}Bu substituted derivatives gave a C_2-symmetric trigonal bipyramidal geometry also for the bismuth species. Hence, the N^{t}Bu-substituted

bismuth species is also predicted to be a pnictogen-centered radical. This change in geometry most likely originates from a combination of steric reasons (*i.e.* due to increased steric bulk of the N^{t}Bu substituents) and electronic factors (*i.e.* a slight change in MO characteristics due to the difference in N-substituent). The optimized geometries of all of the lighter Group 15 congeners are in good agreement with the structures obtained for the NMe derivatives and show only small changes in their calculated hyperfine coupling constants (see Table 2 for values calculated for N^{t}Bu-substituted derivatives [PhB(μ-N^{t}Bu)$_2$]$_2$M$^\bullet$).

This fundamental difference between the electronic structures of the Group 13 radicals [PhB(μ-NR)$_2$]$_2$M$^\bullet$ (M = B, Al, Ga, In) and their group 15 analogs, predicted by the DFT calculations, provided the incentive for investigations of the chemical or electrochemical generation of the pnictogen-centered radicals [PhB(μ-N^{t}Bu)$_2$]$_2$M$^\bullet$ (M = P, As, Sb, Bi).[7]

Synthesis and Chemical Oxidation of LiP[PhB(μ-N^{t}Bu)$_2$]$_2$ (1a): X-ray Structures of 1a and ClP[PhB(μ-NDipp)$_2$] (2). In order to complete the series of bis-*bam* complexes of Group 15 elements of the type LiM[PhB(μ-N^{t}Bu)$_2$]$_2$ (M = P, As, Sb, Bi), and to provide a potential source of the phosphorus-centered radical [PhB(μ-N^{t}Bu)$_2$]$_2$P$^\bullet$, the reaction between PCl_3 and Li_2[PhB(μ-N^{t}Bu)$_2$] was carried out in 1:2 molar ratio.[6] The new phosphorus-containing complex LiP[PhB(μ-N^{t}Bu)$_2$]$_2$ (**1a**) was isolated in 25% yield (Scheme 1) and characterized in solution by multinuclear NMR spectroscopy and in the solid state by a single crystal X-ray structure determination.

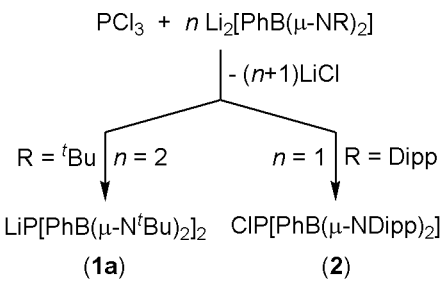

Scheme 1.

The ^{1}H NMR spectrum of **1a** at room temperature in toluene shows a doublet and two singlets in a 1:2:1 intensity ratio for the ^{t}Bu groups and a multiplet for phenyl hydrogens in the expected intensity ratios. The ^{7}Li, ^{11}B and ^{31}P NMR spectra exhibit singlets at 0.94, 34.9 and 87.1 ppm, respectively. The NMR spectroscopic data for **1a** resemble those of the corresponding arsenic complex LiAs[PhB(μ-N^{t}Bu)$_2$]$_2$ (**1b**),[6] suggesting a similar ladder structure for **1a**.

The single crystal X-ray crystallographic analysis confirmed the isostructural nature of **1a** and the heavier Group 15 analogs LiM[PhB(μ-N^{t}Bu)$_2$]$_2$ (M = As, Sb).[6] As illustrated in Figure 2a, the molecular structure of **1a** is comprised of two four-membered rings, BN_2Li and BN_2P, connected by Li-N and P-N bonds to form a tricyclic compound with both three and four-coordinate nitrogens. The B-N bond lengths in **1a** show a slight inequality of *ca.* 0.04 Å (Table 3). Expectedly, the P-N bond to three-coordinate nitrogen is *ca.* 0.12 Å shorter than those involving the four-coordinate nitrogens. The central four-membered PN_2Li ring in **1a** is non-planar with mean torsion angles involving the four atoms of *ca.* 6.5º. The three-coordinate boron and nitrogen atoms in **1a** show a *cis* arrangement with respect to the central four-membered ring similar to that observed in LiM[PhB(μ-N^{t}Bu)$_2$]$_2$ (M = As, Sb).[6]

The oxidation of **1a** with SO_2Cl_2 in both 2:1 and 1:1 molar ratios in diethyl ether was investigated. The attempted one-electron oxidation did not generate an EPR-active species, and both reactions resulted in multiple products. The ^{11}B NMR spectra of the reaction mixtures showed the presence of both three and four-coordinate boron centers, *cf.* formation of **3** described below. The ^{31}P NMR spectra revealed two main products with singlets at 6.0 and -69.9 ppm, comprising *ca.* 70% of the phosphorus-containing compounds; however, no tractable products were isolated from either reaction.

With a view to generating the sterically protected phosphorus-centered radical [PhB(μ-NDipp)$_2$]$_2$P$^{\bullet}$, the reaction between PCl_3 and Li$_2$[PhB(μ-NDipp)$_2$] was conducted in a 1:2 molar ratio.

However, the ^{31}P NMR spectrum revealed a complex mixture of products. Consequently, we decided to attempt installation of the two *bam* ligands on the phosphorus center in a stepwise fashion, a process that had previously been found to be necessary for the successful synthesis of the bis-*bam* aluminum complex $(Et_2O{\cdot}Li)Al[PhB(\mu\text{-}N^tBu)_2]_2$.[4] The reaction between PCl_3 and $Li_2[PhB(\mu\text{-}NDipp)_2]$ in a 1:1 molar ratio produced an 80 % yield of $ClP[PhB(\mu\text{-}NDipp)_2]$ (**2**) (Scheme 1), which was characterized in solution by multinuclear NMR spectroscopy and in the solid state by a single crystal X-ray structure determination. Subsequent reaction between **2** and a second equivalent of $Li_2[PhB(\mu\text{-}NDipp)_2]$, however, also failed to generate the bis-*bam* complex, $LiP[PhB(\mu\text{-}NDipp)_2]_2$.

The ^{1}H NMR spectrum of **2** shows the expected resonances for the phenyl and Dipp groups. The ^{11}B NMR spectrum exhibits a singlet at 32.8 ppm and a single resonance is observed at 189.8 ppm in the ^{31}P NMR spectrum, *cf.* δ (^{31}P) 180 for $ClP[PhB(\mu\text{-}N^tBu)_2]$.[8a] The crystal structure of **2** (Figure 2b) confirms the isostructural relationship with the other structurally characterized Group 15 mono-*bam*s, $XM[PhB(\mu\text{-}N^tBu)_2]$ (X = Br, M = P;X = Cl, M = As, Sb, Bi).[6, 8a] In common with the lighter Group 15 mono-*bam*s, $XM[PhB(\mu\text{-}N^tBu)_2]$ (X = Br, M = P; X = Cl, M = As), **2** does not exhibit the significant intermolecular M···Cl close contacts that were observed for the heavier Group 15 congeners (X = Cl, M = Sb, Bi).[6] The P-N bonds in **2** (Table 3) are somewhat elongated (by *ca.* 0.03 Å) compared to those in the *tert*-butyl derivative $BrP[PhB(\mu\text{-}N^tBu)_2]$,[8a] whereas the B-N bond lengths in **2** are in the typical range for the *bam* ligand.[1] The calculated P-Cl bond order in **2** (0.97)[22] is somewhat higher than the value of *ca.* 0.83 observed for P-Br, As-Cl and Sb-Cl bonds in $XM[PhB(\mu\text{-}N^tBu)_2]$ (X = Br, M = P; X = Cl, M = As, Sb).[6] Steric crowding of the Dipp-groups does not have an effect on the N-P-N and N-P-Cl bond angles as indicated by the similarity of these values with those observed in $BrP[PhB(\mu\text{-}N^tBu)_2]$.[8a] Consistently, the P-N-B and N-B-N angles are also comparable with those observed in $BrP[PhB(\mu\text{-}N^tBu)_2]$.[24]

Chemical Oxidation of LiAs[PhB(μ-N^{t}Bu)$_2$]$_2$ (1b): Synthesis and Characterization of [PhB(μ-N^{t}Bu)$_2$As(μ-N^{t}Bu)$_2$B(Cl)Ph] (3). Since the Group 13 radicals [PhB(μ-N^{t}Bu)$_2$]$_2$M$^\bullet$ (M = Al, Ga) are readily obtained from the corresponding anions by one-electron oxidation with iodine,[4] we initially attempted to generate [PhB(μ-N^{t}Bu)$_2$]$_2$As$^\bullet$ by oxidation of **1b** with half-an-equivalent of I_2, but no reaction was observed. The oxidizing agents [^{n}Bu$_4$N]Br$_3$ and NO[SbF$_6$] were also ineffective. Consequently, we turned our attention to the stronger oxidizing agent sulfuryl chloride. The reaction of a half-equivalent of SO_2Cl_2 with **1b** produced LiCl and an almost colorless reaction solution, suggesting the absence of a radical species. A multinuclear NMR spectroscopic analysis (^{1}H, ^{7}Li, ^{11}B, ^{13}C) of the reaction mixture showed the presence of some unreacted **1b**, as well as a product that exhibits three N^{t}Bu resonances with relative intensities 2:1:1 (^{1}H, ^{13}C), two different environments for boron centers (^{11}B) and no lithium atoms (^{7}Li). Specifically, singlets were observed at 37.3 and 7.6 ppm in the ^{11}B NMR spectrum, suggesting the presence of both three-coordinate and four-coordinate boron atoms, respectively. In the light of these NMR data, the reaction of SO_2Cl_2 with **1b** was carried out in a 1:1 molar ratio and the product [PhB(μ-N^{t}Bu)$_2$As(μ-N^{t}Bu)$_2$B(Cl)Ph] (**3**) was isolated in 85% yield (eq. 1), and identified by an X-ray crystallographic analysis.

LiAs[PhB(μ-N^{t}Bu)$_2$]$_2$ + SO_2Cl_2 → [PhB(μ-N^{t}Bu)$_2$As(μ-N^{t}Bu)$_2$B(Cl)Ph] + LiCl (1)

(**1b**) (**3**)

The crystal structure of **3** with the atomic numbering scheme is depicted in Figure 3a, and the pertinent bond parameters are summarized in Table 4. The structure consists of a spirocyclic arsenic complex in which the arsenic center is *N*,*N*′-chelated by a *bam* ligand and a chlorinated *bam* ligand with B-Cl bond. The solid-state structure is consistent with the observation of both three- and four-coordinate boron centers and three ^{t}Bu environments (bonded to nitrogens N1, N2 and N3/N4,

respectively) in the solution NMR spectra. The B-Cl bond formation in the three atom NBN backbone is a novel feature in the chemistry of boraamidinates.[1] A similar arrangement for four-coordinate boron can be found, however, in amidinate complexes of the Ph(Cl)B unit.[25, 26]

The B-N bonds in the chlorinated *bam* ligand in **3** are *ca*. 0.12 Å longer than those in the non-chlorinated ligand owing to the influence of the four-coordinate boron center in the former. Concomitantly, the As-N bonds involving the chlorinated *bam* ligand are *ca*. 0.07 Å shorter than those in the *bam* ligand. The As-N bond lengths to the *bam* ligand are comparable to those observed in the mono-*bam*, [PhB(μ-N^{t}Bu)$_2$]AsCl (1.839(5) and 1.846(5) Å),[6] while the corresponding bonds to the chlorinated ligand are the shortest reported for the arsenic *bam* complexes thus far; the As-N bond involving the three-coordinate nitrogen in **1b** has a bond length of 1.789(3) Å.[6] These bond lengths are indicative of a Zwitterionic compound with the positive charge located mainly on arsenic and the negative charge on the four-coordinate boron center. The B-Cl bond length of 1.953(4) Å in **3** is significantly longer than those observed in amidinate complexes of the Ph(Cl)B unit (1.847(4)-1.882(6) Å), while the elongated B-N bond distances in **3** are comparable to the corresponding B-N bonds in the amidinate complexes.[25, 26] The lengthened B-N bonds in **3** are, however, among the longest observed in the three atom NBN backbone of the *bam* ligand; similar bond lengths have been reported only when four-coordinate nitrogen atoms are involved.[1]

Elongation of the B-N bonds and contraction of the As-N bonds results in a wider N-As-N angle (*ca*. 5.5º) within the chlorinated ligand and a narrower N-B-N angle (*ca*. 8.1º) at the four-coordinate boron. Although the N-B2-Cl and C-B2-Cl bond angles show ideal tetrahedral values, the remaining bond angles at B2 atom are somewhat distorted due to the involvement of this atom in the four-membered AsNBN ring with a bite angle at boron of 93.8(8)º. The three-coordinate boron atom shows a trigonal planar geometry (sum of bond angles is 359.9º), as is typical for *bam* ligands.[1] The four-membered AsNBN rings are slightly distorted from planarity with torsion angles of *ca*. 2.3 and 4.5º. These two rings are almost perpendicular to each other with an angle of 87.9º between the two

planes. The geometry at the spirocyclic arsonium center is distorted tetrahedral; the NAsN bite angles of 75.7(1)^{o} for the chlorinated *bam* ligand and 81.2(1)^{o} for the *bam* ligand, while the other NAsN bond angles are in the range 125.1(1)-128.7(1)^{o}.[24]

Chemical Reduction of [PhB(μ-N^{t}Bu)$_2$As(μ-N^{t}Bu)$_2$B(Cl)Ph] (3). Since oxidation of **1b** resulted in the formation of **3** via a two-electron process, we turned our attention to the reduction of **3** as a possible route to the radical [PhB(μ-N^{t}Bu)$_2$]$_2$As$^{\bullet}$. Initial attempts to reduce **3** with Ph_3Sb in Et_2O or with metallic sodium in THF were unsuccessful. Consequently, we chose sodium naphthalenide as a stronger reducing agent.[27]

Upon addition of Na[$C_{10}H_8$] to a solution of **3** in THF at -80 ºC, the dark green color of the naphthalenide radical anion disappeared to give a colorless solution. The ^{1}H NMR spectrum of the reaction mixture showed the presence of the compound **3**, naphthalene and a new product with three singlets for the N^{t}Bu-groups at 1.38, 1.29 and 1.20 ppm in a 1:2:1 intensity ratio. The ^{11}B NMR spectrum exhibited a relatively low intensity signal at 7.6 ppm for the four-coordinate boron in **2**, and a broad resonance at *ca.* 36 ppm attributed to the three-coordinate boron atoms in both **2** (37.3 ppm) and the new product. The similarity of the ^{1}H NMR spectrum for the new product and that reported for the known compound LiAs[PhB(μ-N^{t}Bu)$_2$]$_2$ (three resonances at 1.39, 1.30 and 1.22 ppm with a 1:2:1 intensity ratio),[6] suggests that a two-electron reduction with formation of the analogous sodium salt NaAs[PhB(μ-N^{t}Bu)$_2$]$_2$, has occurred (Scheme 2).

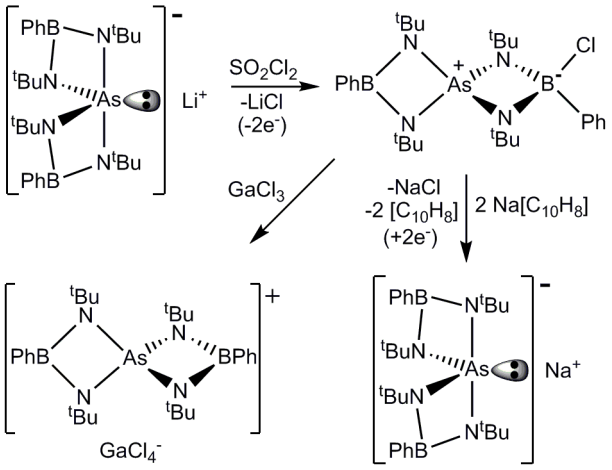

Scheme 2.

Synthesis and Characterization of [PhB(μ-N^{t}Bu)$_2$]$_2$As$^+$GaCl$_4^-$ (4). The chemical or electrochemical reduction of the cation [PhB(μ-N^{t}Bu)$_2$]$_2$As$^+$ represents another potential source of the radical, [PhB(μ-N^{t}Bu)$_2$]$_2$As$^\bullet$. With this target in mind, we prepared the ion-separated salt [PhB(μ-N^{t}Bu)$_2$]$_2$As$^+$GaCl$_4^-$ (**4**) in excellent yield by the reaction of **3** with $GaCl_3$ in diethyl ether (eq. 2). The ^{1}H and ^{11}B NMR spectra of **4** in CD_2Cl_2 reveal a single environment for all four ^{t}Bu groups and a single resonance for three-coordinate boron, consistent with chloride ion abstraction from the B-Cl unit in **3**. The ^{71}Ga NMR spectrum exhibits a single resonance at 249.6 ppm, which is a typical chemical shift for the $GaCl_4^-$ anion.[29]

$$[PhB(\mu\text{-}N^tBu)_2As(\mu\text{-}N^tBu)_2B(Cl)Ph] + GaCl_3 \rightarrow [PhB(\mu\text{-}N^tBu)_2]_2As^+GaCl_4^- \quad (2)$$

(**3**) (**4**)

The crystal structure of **4** exhibits two independent ion pairs in the crystal lattice. Several data collections were attempted, but the second $GaCl_4^-$ anion consistently showed disorder in the chlorine atom positions. The bond parameters of the other $GaCl_4^-$ anion, and both of the two [PhB(μ-N^{t}Bu)$_2$]$_2$As$^+$ cations (Figure 3b), however, display reasonable estimated standard deviations. The

As-N and B-N bond lengths in **4** are intermediate between the values observed for the two ligands in **3** (Table 4). As expected, however, they are somewhat closer to the parameters observed for the *bam* ligand in **3**. The endocyclic N-B-N and N-As-N bond angles in **4** are also close to those observed in the non-chlorinated *bam* ligand in **3**. As observed for Group 13 neutral radicals $[PhB(\mu\text{-}N^tBu)_2]_2M^\bullet$ (M = Al, Ga),[3, 4] the methyl-groups in the ^{t}Bu units of both ligands in **4** are staggered whereas the B-Cl bond formation in **3** results in an eclipsed conformation. The four-membered AsNBN rings in **4** are slightly distorted from planarity with torsion angles of 1.9 and 3.4º, and the angle between these planes is only slightly closer to 90º (88.8º) than that in **3**. Finally, the bond angles in the $GaCl_4^-$ anion are close to those of an ideal tetrahedron.[30]

Electrochemistry of $[PhB(\mu\text{-}N^tBu)_2]_2As^+GaCl_4^-$ (4) and $LiAs[PhB(\mu\text{-}N^tBu)_2]_2$ (1b). Voltammetric studies performed on **4** in acetonitrile showed a single wave which was both chemically and electrochemically irreversible over scan rates of 0.1 – 20 V s^{-1}, on both Pt and GC electrodes. Multiple CVs taken at the same scan rate and concentration, both before and after the addition of ferrocene (as an internal reference), resulted in variations in the cathodic peak current height, as indicated in Figure 4, with essentially invariant peak potentials near -1.3 V. The variation in the magnitude of the peak current for the reduction process can be attributed to adsorption of the radical onto the surface of the electrode. Such adsorption effects have been well documented for thiols on metals such as gold and platinum.[31] Thus, while the peak currents can give no information on the number of electrons transferred, the adsorption phenomenon itself supports a one electron reduction to a reactive radical. The complete absence of a return wave (at an offset potential) suggests that radical dimerization to give an As-As bonded species is not a significant pathway under the conditions used in this study. Radical dimerization has been observed, however, in the one-electron electrochemical reduction of Ph_2AsBr, which produces $Ph_2AsAsPh_2$.[32]

Voltammetric studies performed on **1b** in both dichloromethane and tetrahydrofuran on Pt, GC, and Au electrodes showed at least one oxidation process, which is also chemically and electrochemically irreversible, and takes place near the edge of the solvent window. This initial oxidation process gives rise to a return wave in THF which is offset by 1.5 V on Au (Figure 5), and by over 1.8 V on Pt (these waves are observed only after scanning through the +1.24 V process). The presence of this offset return wave may indicate that, upon oxidation of **1b**, the lithium ion complexes with THF to give $[PhB(\mu\text{-}N^tBu)_2]_2As^\bullet$ and $Li(THF)_4^+$. The intermediacy of such lithium complexes have been implicated previously in related systems.[33] The return wave would then correspond to reduction of the electrochemically generated radical at +1.24 V. Two irreversible oxidation processes occurred in CH_2Cl_2 on GC, Pt, and Au, at +0.9 V and +1.3 V respectively, with no evidence for return waves. The insolubility of **1b** in CH_3CN precluded electrochemical measurements in that solvent.

Comparison of redox potentials for irreversible processes and among different solvent/electrode combinations is fraught with difficulties. Follow-up reactions, whether decomposition or adsorption, can significantly displace apparent $E°$ values. Even with such caveats, these two incompatible sets of peak potentials (i.e., -1.3 V for the 0/+1 couple in **4** and 1.24 V for the -1/0 couple in $LiAs[PhB(\mu\text{-}N^tBu)_2]_2$ (**1b**) indicate that the existence of the neutral radical $[PhB(\mu\text{-}N^tBu)_2]_2As^\bullet$ is likely to be thermodynamically unfavorable. Insofar as they do reflect the redox transformations of $[Asbam_2]^y$ (y = -1, 0, +1), it appears that the strong complexation of lithium in **1b** has a powerful stabilizing effect. Thus, the onset of oxidation of this species is found at least several volts more anodic than observed for the y = 0/+1 couple in **4**.

Attempts to generate the radical $[PhB(\mu\text{-}N^tBu)_2]_2As^\bullet$ by SEEPR, an *in situ* method optimized for the detection of short-lived, electrochemically generated radicals,[10] by reductive electrolysis of **4** at -1.3 V in CH_3CN or oxidative electrolysis of **1b** at +0.9 V in CH_2Cl_2 or at 1.3 V in THF did not produce a detectable EPR-active species.

Conclusions.

Intriguingly, DFT calculations predict that the formal addition of two electrons to the neutral Group 13 radicals $[PhB(\mu\text{-}N^tBu)_2]_2M^\bullet$ (M = Al, Ga, In) to give the corresponding Group 15 systems $[PhB(\mu\text{-}N^tBu)_2]_2M^\bullet$ (M = P, As, Sb, Bi) results in a dramatic change in the electronic structure from one in which the unpaired electron density is equally localized on the four nitrogen atoms of the two *bam* ligands to systems that can be described as pnictogen-centered radicals. Oxidation of the anion $[PhB(\mu\text{-}N^tBu)_2]_2As^-$ with sulfuryl chloride resulted in B-Cl bond formation, the first example of reactivity at the boron centre in *bam* complexes,[1] and the subsequent characterization of the spirocyclic cation $[PhB(\mu\text{-}N^tBu)_2]_2As^+$ isoelectronic with the neutral germanium spirocycle $[PhB(\mu\text{-}N^tBu)_2]_2Ge$.[34] Investigations of the chemical redox behavior of the $[PhB(\mu\text{-}N^tBu)_2]_2As^-$ anion and the $[PhB(\mu\text{-}N^tBu)_2]_2As^+$ cation showed that a two-electron process is favored over a one-electron process. Although the voltammetric studies suggest one-electron processes, no direct evidence for the independent existence of the $[PhB(\mu\text{-}N^tBu)_2]_2As^\bullet$ radical was obtained by SEEPR experiments.

Acknowledgments. The authors gratefully acknowledge financial support from the Natural Sciences and Engineering Research Council (Canada), the Alberta Ingenuity Fund (T.L.R. and A.M.C.), and the Academy of Finland (H.M.T.).

Supporting information available: X-ray crystallographic files in CIF format. This material is available free of charge via the Internet at http://pubs.acs.org.

References and Notes

(1) For a recent review, see Fedorchuk, C.; Copsey, M. C.; Chivers, T. *Coord. Chem. Rev*. **2007**, *251*, 897.

(2) Manke, D. R.; Nocera, D. G. *Inorg. Chem*. **2003**, *42*, 4431.

(3) Chivers, T.; Fedorchuk, C.; Schatte, G.; Parvez., M. *Inorg. Chem*. **2003**, *42*, 2084.

(4) Chivers, T.; Eisler, D. J.; Fedorchuk, C.; Schatte, G.; Tuononen, H. M.; Boeré, R. T. *Chem. Commun*. **2005**, 3930.

(5) Chivers, T.; Eisler, D. J.; Fedorchuk, C.; Schatte, G.; Tuononen, H. M.; Boeré, R. T. *Inorg. Chem*. **2006**, *45*, 2119.

(6) Konu, J.; Balakrishna, M. S.; Chivers, T.; Swaddle, T. W. *Inorg. Chem.*, **2007**, *46*, 2627.

(7) In this paper, the term "pnictogen" refers to the central, heavy group 15 element (P, As, Sb, Bi) in all spirocyclic complexes.

(8) (a) Chivers, T.; Fedorchuk, C.; Schatte, G.; Brask, J. K. *Can. J. Chem*. **2002**, *80*, 821; (b) Chivers, T.; Fedorchuk, C.; Parvez, M. *Inorg. Chem.*, **2004**, *43*, 2643.

(9) Jolly, W. L. *The Synthesis and Characterization of Inorganic Compounds*; Prentice Hall: Englewood Cliffs, NJ, 1970; p. 484.

(10) Boeré, R. T.; Bond, A. M.; Chivers, T.; Feldberg, S. W.; Roemmele, T. L. *Inorg. Chem.* **2007**, *46*, 5596.

(11) Sheldrick, G. M. SHELXS-97, *Program for Crystal Structure Determination*, University of Göttingen, Germany, **1997**.

(12) Sheldrick, G. M. SHELXL-97, *Program for Crystal Structure Refinement*, University of Göttingen, Germany, **1997**.

(13) (a) Perdew, J. P.; Burke, K.; Ernzerhof, M. *Phys. Rev. Lett.* **1996**, *77*, 3865. (b) Perdew, J. P.; Burke, K.; Ernzerhof, M. *Phys. Rev. Lett.* **1997**, *78*, 1396. (c) Perdew, J. P.; Ernzerhof, M.; Burke, K. *J. Chem. Phys.* **1996,** *105*, 9982. (d) Ernzerhof, M.; Scuseria, G. E. *J. Chem. Phys.* **1999**, *110*, 5029.

(14) The basis sets were used as they are referenced in the Turbomole 5.9.1 internal basis set library. See ftp://ftp.chemie.uni-karlsruhe.de/pub/ for explicit basis set listings.

(15) Bergner, A.; Dolg, M.; Kuechle, W.; Stoll, H.; Preuss, H. *Mol. Phys.* **1993**, *80*, 1431.

(16) a) TURBOMOLE, Program Package for *ab initio* Electronic Structure Calculations, Version 5.9.1 Theoretical Chemistry Group, University of Karlsruhe, Karlsruhe, Germany, 2007; b) Ahlrichs, R.; Bär, M.; Häser, M.; Horn, H; Kölmel, C. *Chem. Phys. Lett.* **1989**, *162*, 165.

(17) Frisch, M. J.; Trucks, G. W.; Schlegel, H. B.; Scuseria, G. E.; Robb, M. A.; Cheeseman, J. R.; Montgomery, Jr., J. A.,; Vreven, T.; Kudin, K. N.; Burant, J. C.; Millam, J. M.; Iyengar, S. S.; Tomasi, J.; Barone, V.; Mennucci, B.; Cossi, M.; Scalmani, G.; Rega, N.; Petersson, G. A.; Nakatsuji, H.; Hada, M.; Ehara, M.; Toyota, K.; Fukuda, R.; Hasegawa, J.; Ishida, M.; Nakajima, T.; Honda, Y.; Kitao, O.; Nakai, H.; Klene, M.; Li, X.; Knox, J. E.; Hratchian, H. P.; Cross, J. B.; Adamo, C.; Jaramillo, J.; Gomperts, R.; Stratmann, R. E.; Yazyev, O.; Austin, A. J.; Cammi, R.; Pomelli, C.; Ochterski, J. W.; Ayala, P. Y.; Morokuma, K.; Voth, G. A.; Salvador, P.; Dannenberg, J. J.; Zakrzewski, V. G.; Dapprich, S.; Daniels, A. D.; Strain, M. C.; Farkas, O.; Malick, D. K.; Rabuck, A. D.; Raghavachari, K.; Foresman, J. B.; Ortiz, J. V.; Cui, Q.; Baboul, A. G.; Clifford, S.; Cioslowski, J.; Stefanov, B. B.; Liu, G.; Liashenko, A.; Piskorz, P.; Komaromi, I.; Martin, R. L.; Fox, D. J.; Keith, T.; Al-Laham, M. A.; Peng, C. Y.; Nanayakkara, A.; Challacombe, M.; Gill, P. M. W.; Johnson, B.; Chen, W.; Wong, M. W.; Gonzalez, C.; Pople, J. A *Gaussian 03*, (Revision C.02), Gaussian, Inc., Pittsburgh, PA, **2003**.

(18) (a) van Lenthe, E.; Baerends, E. J.; Snijders, J. G. *J. Chem. Phys.* **1993**, *99*, 4597. (b) van Lenthe, E.; Baerends, E. J.; Snijders, J. G. *J. Chem. Phys.* **1994**, *101*, 9783. (c) van Lenthe, E.; Ehlers, A. E.; Baerends, E. J. *J. Chem. Phys.* **1999**, *110*, 8943.

(19) (a) van Lenthe, E.; Baerends, E. J. *J. Comp. Chem.* **2003**, *24*, 1142. (b) Chong, D. P.; Lenthe, E.; van Gisbergen, S. J. A.; Baerends, E. J. *J. Comp. Chem.* **2004**, *25*, 1030.

(20) ADF2007.01, SCM, Theoretical Chemistry, Vrije Universiteit, Amsterdam, Netherlands, http://www.scm.com.

(21) Although the product was spectroscopically pure, on the basis of multinuclear (^{1}H, ^{13}C, ^{11}B) NMR spectra, numerous attempts, by both in-house and commercial services, gave unsatisfactory elemental analyses.

(22) The P-Cl bond order was calculated by the Pauling equation $N = 10^{(D-R)/0.71}$,[23] where R is the observed bond length (Å). The single bond length D is estimated from the sums of appropriate covalent radii (Å):[23] P-Cl 2.09.

(23) Pauling, L. *The Nature of the Chemical Bond*; 3rd Ed.; Cornell University Press; Ithaca, NY, **1960.**

(24) In view of the multiple products detected by ^{31}P NMR spectroscopy after chemical oxidation of **1a** and the difficulties involved in the purification of the antimony derivative LiSb[PhB(μ-N^{t}Bu)$_2$]$_2$ due to the co-formation of the 2:3 complex, Sb$_2$[PhB(μ-N^{t}Bu)$_2$]$_3$,[6] we have focused our attempts to generate Group 15-centered radicals of the type [PhB(μ-N^{t}Bu)$_2$]$_2$M$^{\bullet}$ on the arsenic system **1b**. The oxidation of (Et$_2$O·Li)Bi[PhB(μ-N^{t}Bu)$_2$]$_2$ with iodine or SO_2Cl_2, however, was conducted and resulted in the formation of a mixture of the known 2:3 *bam* complex, Bi$_2$[PhB(μ-N^{t}Bu)$_2$]$_3$,[6] and a number of unidentified compounds.

(25) Blais, P.; Chivers, T.; Downard, A.; Parvez, M. *Can. J. Chem.*, **2000**, *78*, 10.

(26) Findlater, M.; Hill, N. J.; Cowley, A. H. *Polyhedron*, **2006**, *25*, 983.

(27) Metallic sodium has a formal reduction potential of -3.04 V (*vs.* Fc) in THF or glyme, while the formal reduction potential for the naphthalenide radical anion is -3.10 V (*vs.* Fc) in THF.[28]

(28) Connelly, N. G.; Geiger, W. E. *Chem. Rev.*, **1996**, *96*, 877, and references therein.

(29) See for example Cowley, A. H; Carrano, C. J.; Geerts, R. L.; Jones, R. A.; Nunn, C. M. *Angew. Chem., Int. Ed. Engl.*, **1988**, *27*, 277.

(30) The one-electron reduction of **4** with Cp$_2$Co was attempted in diethyl ether at -80 ^{o}C. The deep red color of Cp$_2$Co disappeared immediately upon dropwise addition of the reducing

agent; no EPR-active species could be detected. The ^{1}H NMR spectrum revealed a complex mixture of products none of which could be isolated.

(31) (a) Finklea, H. O. *Electrochemistry of Organized Monolayers of Thiols and Related Molecules on Electrodes.* Electroanalytical Chemistry; Bard, A. J.; Rubinstein, I., Eds.; Marcel Dekker: New York, 1996. (b) Lipkowski, J.; Ross, P. N., Eds. *Adsorption of Molecules at Metal Electrodes*; VCH: New York, 1992. (c) Mazur, M.; Krysinski, P. *J. Phys. Chem. B,* **2002**, *106*, 10349.

(32) Dessy, R. E.; Chivers, T.; Kitching, W. *J. Am. Chem. Soc*. **1965**, *88*, 467.

(33) (a) Armstrong, A..; Chivers, T.; Parvez, M.; Boeré, R. T. *Angew. Chem., Int. Ed. Engl.* **2004**, *43*, 502. (b) Armstrong, A.; Chivers, T.; Parvez, M.; Schatte, G.; Boeré, R. T. *Inorg. Chem.* **2004**, *43*, 3453. (c) Armstrong, A.; Chivers, T.; Tuononen, H. M.; Parvez, M.; Boeré, R. T. *Inorg. Chem.* **2005**, *44*, 7981.

(34) Konu, J; Chivers, T. unpublished results.

Table 1. Crystallographic data for LiP[PhB(μ-N^{t}Bu)$_2$]$_2$ (**1a**), ClP[PhB(μ-NDipp)$_2$] (**2**), [PhB(μ-N^{t}Bu)$_2$As(μ-N^{t}Bu)$_2$B(Cl)Ph] (**3**) and [PhB(μ-N^{t}Bu)$_2$]$_2$As$^+$GaCl$_4^-$ (**4**).[a]

	1a	**2**	**3**	**4**
empirical formula	$C_{28}H_{46}B_2LiN_4P$	$C_{30}H_{39}BClN_2P$	$C_{28}H_{46}AsB_2ClN_4$	$C_{28}H_{46}AsB_2Cl_4GaN_4$
fw	498.22	504.86	570.68	746.75
cryst. system	monoclinic	monoclinic	monoclinic	monoclinic
space group	C*2/c*	P*2$_1$/c*	P*2$_1$/n*	P*2$_1$/n*
a, Å	25.993(5)	15.876(3)	10.700(2)	10.690(2)
b, Å	8.674(2)	12.416(3)	16.593(3)	37.733(8)
c, Å	18.342(4)	15.917(4)	17.521(4)	18.605(4)
α, deg.	90.00	90.00	90.00	90.00
β, deg.	134.55(3)	115.22(3)	100.83(3)	91.31(3)
γ, deg.	90.00	90.00	90.00	90.00
V, Å^3	2947(2)	2839(1)	3055(1)	7503(3)
Z	4	4	4	8
T, ^{o}C	-100	-100	-100	-100
ρ_{calcd}, g/cm^3	1.123	1.181	1.241	1.322
μ(Mo Kα), mm^{-1}	0.116	0.212	1.223	1.917
crystal size, mm^3	0.12x0.06x0.02	0.10x0.08x0.06	0.24x0.20x0.02	0.20x0.12x0.08
F(000)	1080	1080	1208	3072
Θ range, deg	3.40-25.03	3.27-25.03	3.47-25.03	2.18-25.03
reflns collected	4614	15549	8669	22880
unique reflns	2578	4804	5343	13105
R_{int}	0.0228	0.0539	0.0352	0.0511
reflns [$I>2\sigma(I)$]	2200	3679	3999	8641
R_1 [$I>2\sigma(I)$] [b]	0.0641	0.0435	0.0435	0.0598
wR_2 (all data) [c]	0.1875	0.1100	0.1014	0.1494
GOF on F^2	1.084	1.019	1.048	1.015
completeness	0.993	0.960	0.990	0.989

[a] λ (MoKα) = 0.71073 Å. [b] $R_1 = \Sigma \big| |F_o| - |F_c| \big| / \Sigma |F_o|$. [c] $wR_2 = [\Sigma w(F_o^2-F_c^2)^2/\Sigma wF_o^4]^{½}$.

Table 2. Calculated Hyperfine Coupling Constants for [PhB(μ-N^{t}Bu)$_2$]$_2$M$^\bullet$ [G]

	n[a]	**M = ^{31}P**	**M = ^{75}As**	**M = ^{121}Sb**	**M = ^{209}Bi**
^{11}B	2	-1.9	-3.7	-3.9	-5.6
^{14}N	2	12.8	11.4	9.3	6.2
^{14}N	2	-1.8	-2.0	-2.0	-0.1
M	1	514.4	491.4	758.0	572.4

[a] Number of equivalent nuclei.

Table 3. Selected bond lengths (Å) and angles (°) in LiP[PhB(μ-N^{t}Bu)$_2$]$_2$ (**1a**) and ClP[PhB(μ-NDipp)$_2$] (**2**).

	1a	**2**		**1a**	**2**
P1-N1	1.690(4)	1.713(2)	B1-N2	1.455(4)	1.455(3)
P1-N2	1.834(4)	1.716(2)	Li1^a-N2	1.97(2)	-
P1-X	1.789(4)^b	2.099(1)^c	Li1^a-N1^a	1.76(3)	-
B1-N1	1.416(4)	1.447(3)	Li1^a-N2^a	2.01(3)	-
N1-P1-N2	111.1(2)	79.4(1)	P1-N1-B1	83.5(2)	91.0(1)
N1-P1-X	83.5(2)^b	103.4(1)^c	P1-N2^a-B1	78.9(2)	90.6(1)^d
N2-P1-X	103.8(1)^b	104.2(1)^c	N1^a-B1^a-N2	107.7(2)	-
N1-B1-N2^a	107.7(2)	98.0(2)^d	B1^a-N2-P1	125.2(2)	-

^{a} Symmetry operation: -x, y, 0.5-z. ^{b} X = N2^a. ^{c} X = Cl1. ^{d} no symmetry operation on N2 atom.

Table 4. Selected bond lengths (Å) and angles (°) in [PhB(μ-N^{t}Bu)$_2$As(μ-N^{t}Bu)$_2$B(Cl)Ph] (**3**) and [PhB(μ-N^{t}Bu)$_2$]$_2$As$^+$GaCl$_4^-$ (**4**).

	3	**4**[a]		**3**	**4**[a]
As1-N1	1.825(3)	1.800(4)	B2-N4	1.569(5)	1.469(7)
As1-N2	1.833(3)	1.811(4)	B2-Cl1	1.953(4)	-
As1-N3	1.755(3)	1.803(4)	Ga-Cl1	-	2.176(2)
As1-N4	1.764(3)	1.797(4)	Ga-Cl2	-	2.171(2)
B1-N1	1.441(5)	1.466(7)	Ga-Cl3	-	2.194(4)
B1-N2	1.448(5)	1.453(7)	Ga-Cl4	-	2.175(2)
B2-N3	1.565(5)	1.453(7)			
	3	**4**[a]		**3**	**4**[a]
N1-As1-N2	75.7(1)	77.7(2)	N3-B2-C200	116.7(3)	-
N1-As1-N3	127.1(1)	129.3(2)	N4-B2-C200	117.9(3)	-
N1-As1-N4	126.6(1)	128.4(2)	Cl1-B2-C200	109.4(3)	-
N2-As1-N3	125.1(1)	125.0(2)	Cl1-Ga1-Cl2	-	107.52(8)
N2-As1-N4	128.7(1)	126.4(2)	Cl1-Ga1-Cl3	-	109.60(7)
N3-As1-N4	81.2(1)	77.8(3)	Cl1-Ga1-Cl4	-	110.66(8)
N1-B1-N2	101.9(3)	101.7(4)	Cl2-Ga1-Cl3	-	111.18(8)
N3-B2-N4	93.8(8)	101.3(4)	Cl2-Ga1-Cl4	-	108.55(8)
N3-B2-Cl1	108.9(3)	-	Cl3-Ga1-Cl4	-	109.32(7)
N4-B2-Cl1	109.2(2)	-			

[a] Bond parameters of the second discrete ion pair are identical.

Figure Captions

Figure 1. SOMOs (isosurface value ± 0.06) of the neutral $[PhB(\mu\text{-}NMe)_2]_2M^{\bullet}$ radicals; (a) M = P, As, Sb, (b) M = Bi. Electronic structures of the ^{t}Bu-derivatives, $[PhB(\mu\text{-}N^{t}Bu)_2]_2M^{\bullet}$ (M = P, As, Sb, Bi), are analogous to that presented in Figure 1a.

Figure 2. Crystal structures of (a) $LiP[PhB(\mu\text{-}N^{t}Bu)_2]_2$ (**1a**), and (b) $ClP[PhB(\mu\text{-}NDipp)_2]_2$ (**2**) with the atomic numbering scheme. Hydrogen atoms have been omitted for clarity. [a] Symmetry operation: -x, y, 0.5-z.

Figure 3. (a) Molecular structure of $[PhB(\mu\text{-}N^{t}Bu)_2As(\mu\text{-}N^{t}Bu)_2B(Cl)Ph]$ (**3**), and (b) crystal structure of the $[PhB(\mu\text{-}N^{t}Bu)_2]_2As^{+}$ cation in **4** with the atomic numbering schemes. Hydrogen atoms have been omitted for clarity. Only one of the two independent cations is shown in **4**.

Figure 4. Cyclic voltammograms of **4** (1.7 mM) and ferrocene (2.7 mM) in CH_3CN at a GC electrode at 21 °C, $[^{n}Bu_4N][PF_6]$ (0.1 M), ν = 0.2 V s^{-1}: (a) immediately after the addition of ferrocene, (b) before the addition of ferrocene, and (c) several minutes after the addition of ferrocene.

Figure 5. Cyclic voltammogram of **1b** (1.4 mM) and ferrocene (0.6 mM) in THF at a Au electrode at 21 °C, $[^{n}Bu_4N][PF_6]$ (0.4 M), ν = 0.2 V s^{-1}.

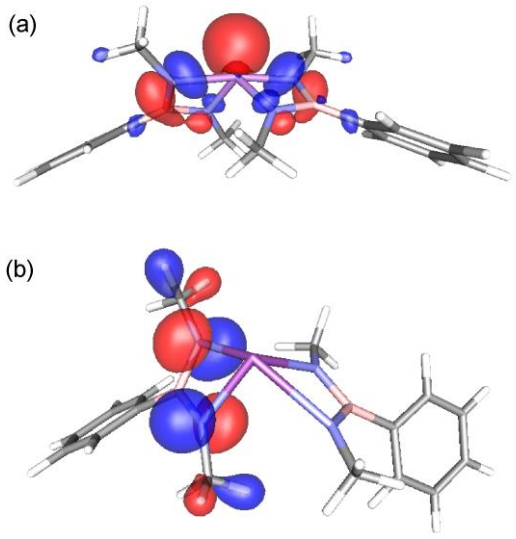

Figure 1.

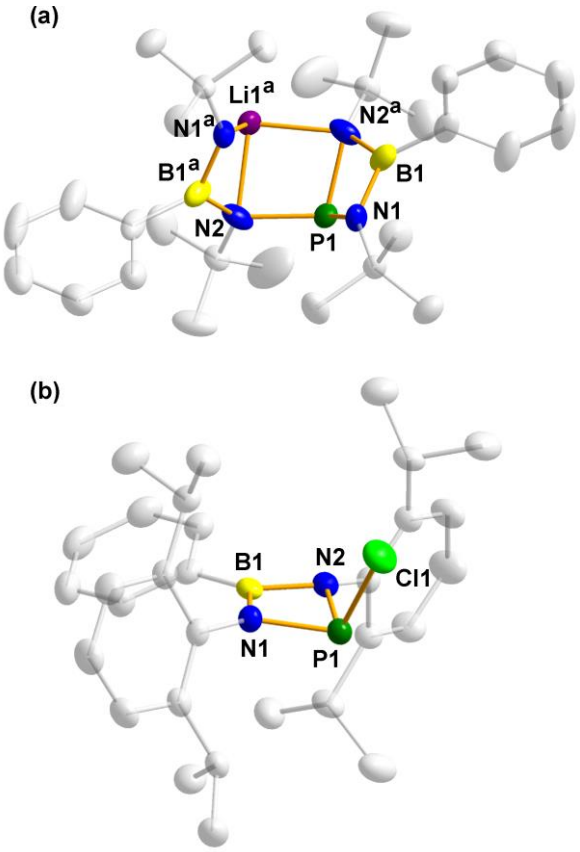

Figure 2.

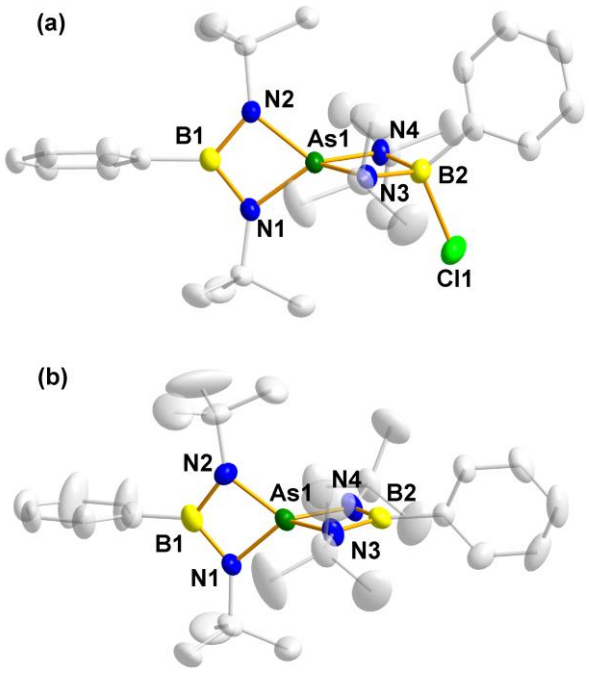

Figure 3.

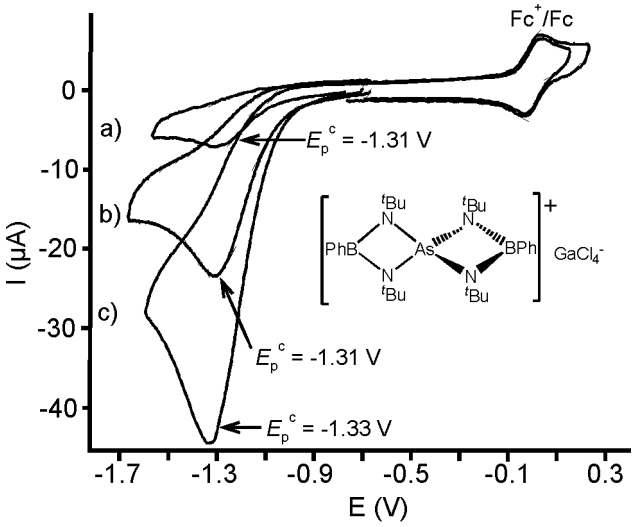
Fc+/Fc
0
-10
-20
-30
-40
I (μA)
a)
b)
c)
Ep c = -1.31 V
Ep c = -1.31 V
Ep c = -1.33 V
tBu
N
PhB
As
BPh
GaCl4-
+
-1.7
-1.3
-0.9
-0.5
-0.1
0.3
E (V)

Figure 4.

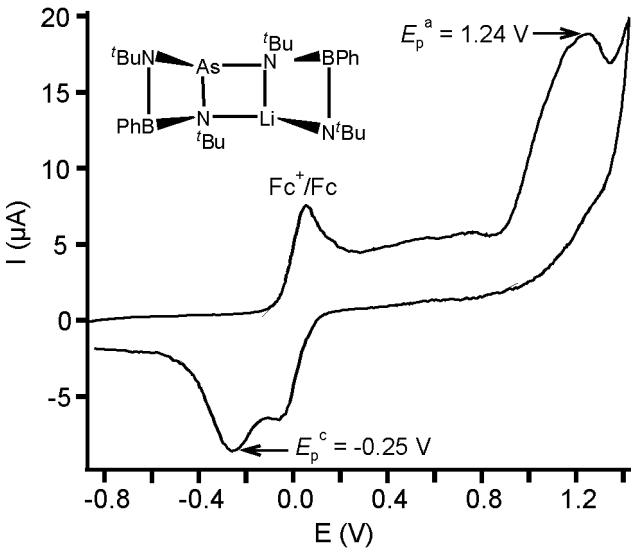
20
15
10
5
0
-5
I (μA)
-0.8
-0.4
0.0
0.4
0.8
1.2
E (V)
E_p^a = 1.24 V
E_p^c = -0.25 V
Fc+/Fc
tBuN
As
tBu
N
BPh
PhB
N
tBu
Li
NtBu

Figure 5.